

NO-A181 271

BIF(AO+ V') RADIATIVE LIFETIMES AND RATE COEFFICIENTS
FOR V YIELDS T TRAN. (U) AEROSPACE CORP EL SEGUNDO CA
AEROPHYSICS LAB R F HEIDNER ET AL. 24 APR 87
TR-8884A(5938-81)-6 SD-TR-87-19

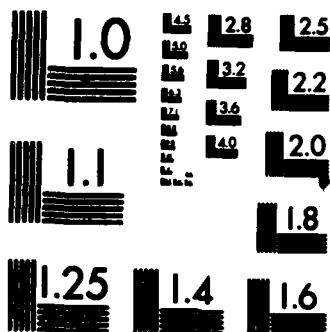
1/1

UNCLASSIFIED

F/G 28/8

NL





MICROCOPY RESOLUTION TEST CHART
NATIONAL BUREAU OF STANDARDS-1963-A

DTIC FILE COPY

12

**BiF(AO⁺, v') Radiative Lifetimes and
Rate Coefficients for V ↔ T Transfer
and Electronic Quenching**

R. F. HEIDNER III, H. HELVAJIAN,
J. S. HOLLOWAY, and J. B. KOFFEND
Aerophysics Laboratory
Laboratory Operations
The Aerospace Corporation
El Segundo, CA 90245

DTIC
ELECTE
JUN 04 1987
S D

AD-A181 271

24 April 1987

Prepared for
SPACE DIVISION
AIR FORCE SYSTEMS COMMAND
Los Angeles Air Force Station
P.O. Box 92960, Worldway Postal Center
Los Angeles, CA 90009-2960

APPROVED FOR PUBLIC RELEASE;
DISTRIBUTION UNLIMITED

UNCLASSIFIED

SECURITY CLASSIFICATION OF THIS PAGE (When Data Entered)

REPORT DOCUMENTATION PAGE		READ INSTRUCTIONS BEFORE COMPLETING FORM
1. REPORT NUMBER SD-TR-87-19	2. GOVT ACCESSION NO. AD-A111371	3. RECIPIENT'S CATALOG NUMBER
4. TITLE (and Subtitle) BiF(AO ⁺ ,v') Radiative Lifetimes and Rate Coefficients for V-T Transfer and Electronic Quenching		5. TYPE OF REPORT & PERIOD COVERED
7. AUTHOR(s) R. F. Heidner III, H. Helvajian, J. S. Holloway, and J. B. Koffend		6. PERFORMING ORG. REPORT NUMBER TR-0084A(5930-01)-6
8. PERFORMING ORGANIZATION NAME AND ADDRESS The Aerospace Corporation El Segundo, CA 90245		9. CONTRACT OR GRANT NUMBER(s) F04701-84-C-0085
11. CONTROLLING OFFICE NAME AND ADDRESS Space Division Los Angeles Air Force Station Los Angeles, CA 90009-2960		10. PROGRAM ELEMENT, PROJECT, TASK AREA & WORK UNIT NUMBERS
14. MONITORING AGENCY NAME & ADDRESS (if different from Controlling Office)		12. REPORT DATE 24 April 1987
		13. NUMBER OF PAGES 22
		15. SECURITY CLASS. (of this report) Unclassified
		15a. DECLASSIFICATION/DOWNGRADING SCHEDULE
16. DISTRIBUTION STATEMENT (of this Report) Approved for public release; distribution unlimited.		
17. DISTRIBUTION STATEMENT (of the abstract entered in Block 20, if different from Report)		
18. SUPPLEMENTARY NOTES This work was performed under U.S. Air Force Space Division Contract No. F04701-84-C-0085 from 1 October 1984 through 30 September 1985.		
19. KEY WORDS (Continue on reverse side if necessary and identify by block number) Gas phase, rates Electronic state, BiFO Electronic quenching Radiative, lifetime Vibrational, distribution MICRO		
20. ABSTRACT (Continue on reverse side if necessary and identify by block number) The radiative lifetime for several vibrational states (v'=0-3) was measured for electronically excited BiF(AO ⁺). The measured radiative lifetime is 1.4 μ s and does not vary for the v' levels investigated. Also measured for those v' levels are the electronic quenching and V-T rate coefficients for the rare gases He and Ar at an experimental temperature of 485 K. The results indicate Ar is slightly more efficient in electronic quenching than is He. For both gases the quenching rate constants increase with v', and the rates become competitive with the radiative decay rate for pressures in		

DD FORM 1473
(FACSIMILE)UNCLASSIFIED
SECURITY CLASSIFICATION OF THIS PAGE (When Data Entered)

UNCLASSIFIED

SECURITY CLASSIFICATION OF THIS PAGE(When Data Entered)

18. KEY WORDS (Continued)

19. ABSTRACT (Continued)

cont'd → excess of 40 Torr. The vibrational relaxation (V-T) rate constant for all levels studied is at least an order of magnitude greater than those for electronic quenching. The reported V-T rate coefficients scale as $V^{1.7}$ for both He and Ar for $v' = 0$ to $v' = 3$, a result that is contrary to the behavior predicted by the classical harmonic oscillator model.

(Keyman 6)

UNCLASSIFIED

SECURITY CLASSIFICATION OF THIS PAGE(When Data Entered)

PREFACE

We thank J. Herbelin for his support through innumerable enlightening discussions and for serving as an impetus for this experiment.



Accession For	
NTIS CRA&I	<input checked="checked" type="checkbox"/>
DTIC TAB	<input type="checkbox"/>
Unannounced	<input type="checkbox"/>
Justification	
By	
Distribution /	
Availability Codes	
Dist	Avail and/or Special
A-1	

CONTENTS

PREFACE.....	1
I. INTRODUCTION.....	7
II. EXPERIMENTAL.....	9
III. RESULTS.....	13
A. B1F AO ⁺ RADIATIVE LIFETIME.....	13
B. B1F AO ⁺ STATE KINETICS.....	13
IV. DISCUSSION.....	19
A. B1F AO ⁺ RADIATIVE LIFETIME.....	19
B. B1F AO ⁺ STATE KINETICS.....	20
V. SUMMARY.....	25
REFERENCES.....	27

FIGURES

1.	Schematic diagram of the experimental apparatus.....	10
2.	$\text{BiF}(\text{AO}^+, v' = 0 \rightarrow \text{XO}^+, v'' = 2)$ radiative decay at 30 mTorr He and corresponding single exponential fit.....	14
3.	Time evolution profiles of $\text{BiF}(\text{AO}^+, v' = 0, 1, 2, 3)$ fluorescence following initial excitation to $v' = 1$ at $t = 0$ and their associated numerical fits.....	17
4.	Measured $V\text{-}T(k_{i,i-1})$ energy transfer rate coefficients as a function of v' for He and Ar.....	23

TABLE

I.	Radiative Lifetimes, Electronic Quenching Rate Coefficients, and $V\text{-}T$ Relaxation Rate Coefficients for $\text{BiF}(\text{AO}^+)$	14
----	--	----

I. INTRODUCTION

Bismuth monofluoride was first observed in emission (415-510 nm) by Howell, using a high-frequency electrical discharge in BiF_3 vapor.¹ Morgan² independently observed the same radical in absorption (417-487 nm). Since then, the visible band system in BiF has been reinvestigated with much higher resolution,³⁻⁵ was found to follow Hund's case (c) coupling, and has been assigned to the $\text{AO}^+ \leftarrow \text{X}_1\text{O}^+$ electronic transition. Although the A and X states have been well characterized spectroscopically, comparatively few kinetic studies have been conducted on the BiF molecule. Recent investigations in a reactive flow tube apparatus have demonstrated that it is possible to chemically produce large densities of electronically excited BiF AO^+ radicals.⁶ These results have generated interest in developing a chemically pumped $\text{BiF A} \rightarrow \text{X}$ laser with emission at a number of lines near 457 nm. The BiF(A) formation was postulated to occur via sequential collisions of the metastable $\text{NF(a}^1\Delta)$ state with ground-state BiF molecules, a chemical pumping scheme made efficient by the large densities of NF(a) that can be maintained through a chain reaction involving NF_2 and H_2 .^{7,8}

The development of a $\text{BiF A} \rightarrow \text{X}$ chemical laser will require an understanding of the kinetics of the BiF AO^+ and X_1O^+ states. The reactions of NF(a) with the ground X_1O^+ or the intermediate bO^+ metastable states have been described only briefly.⁶ Prior to the present study, virtually nothing was known about the radiative lifetime and kinetics of the AO^+ state. The A state small vibrational spacing (384 cm^{-1}) is such that V-T energy transfer processes are expected to be rapid at room temperature and above. In the reactive flow tube experiments,⁶ it was not possible to accurately measure the AO^+ radiative lifetime, although it was estimated to lie between 10^{-6} and 10^{-7} s.

In this report, we describe experiments in which a tunable, pulsed dye laser is used to excite selected A state vibronic levels. By monitoring the time resolved emission from laser-excited AO^+, v' under collisionless conditions, we have determined the radiative lifetimes for several AO^+ vibrational

states ($v' = 0-3$). By adding buffer gas and monitoring the emission from adjacent vibronic levels and the pumped level, we have obtained the rate coefficients for electronic quenching $k_{q,v'}$, and vibrational-to-translational relaxation (V-T), $k_{v',v'-1}$, by He and Ar.

II. EXPERIMENTAL

The experimental apparatus is depicted schematically in Fig. 1. The BiF was produced using a Broida-type^{9,10} oven mounted in a water-cooled chamber. An alumina crucible containing bismuth metal is mounted within a tungsten basket and heated to temperatures up to 1000 K. At such temperatures, bismuth vapor contains approximately equal concentrations of Bi and Bi₂ ($\sim 10^{14}$ molec cm⁻³).¹¹ The vapor is entrained in a flow of He or Ar from a ring injector and swept up through the conical crucible cap, where it is mixed with a 10% F₂/He mixture at the cone exit. The resulting flame is blue to the eye, and the emission extends from 410 to 810 nm. The majority of the blue emission can be attributed to the BiF A0⁺ + X₁0⁺ system;³ chemiluminescent features in the red can be assigned to the A₁0⁺ + b0⁺ band system.¹² The Bi atomic line at 874 nm is also observed in the flame.¹³ The mechanism for BiF^{*} production is not known, but the direct reactions Bi₂ + F₂, Bi + F₂, and Bi₂ + F can be ruled out due to energetic considerations.¹⁴ This weak background emission does not disturb the experiment, because pulsed laser excitation and time resolved detection were used in the study of the BiF A state kinetics. With this apparatus, a diluent pressure of at least 2 Torr was required to maintain a steady BiF signal.

The BiF A0⁺ radiative lifetime experiments required a substantially lower pressure to attain single-collision conditions. For these experiments, the Broida-type oven was replaced by a stainless-steel boat heater that served to vaporize the bismuth metal. A slow flow of the F₂/He oxidant was directed near the surface of the molten metal to produce the BiF. Pressures as low as 20 mTorr were possible with this system. At that pressure, the mean time between collisions is ~ 5 μ s, which is greater than the A state radiative lifetime reported below.

The gas flows were measured with calibrated (Matheson 601 and 603) flowmeters, and the F₂/He flow was kept much smaller (25 scc min⁻¹) than that of the buffer gas (0.5-5 sl min⁻¹) to avoid further reaction of BiF with F₂ to form BiF_n. Indeed, the BiF signals were very sensitive to the F₂/He flow rate

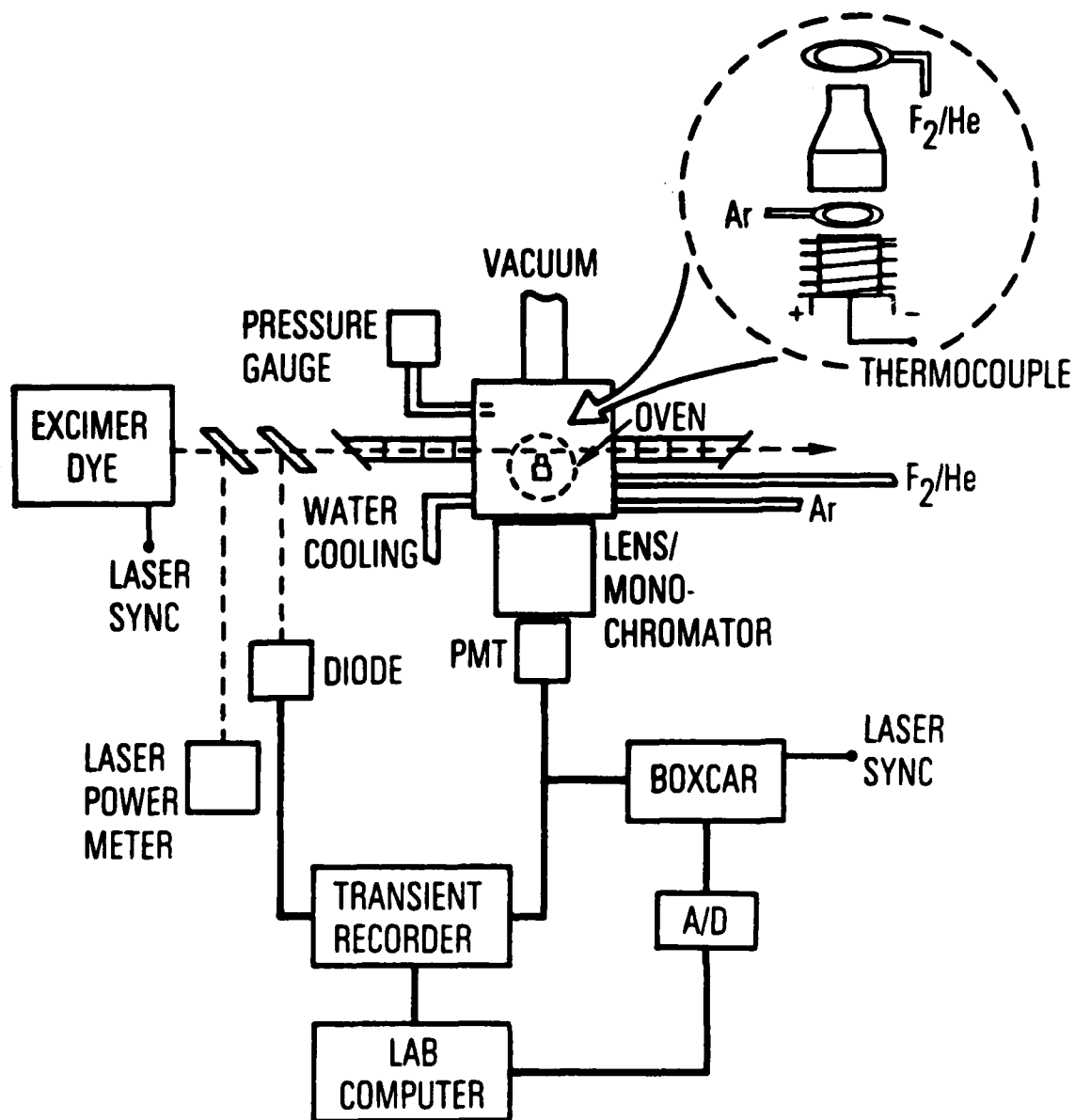


Fig. 1. Schematic diagram of the experimental apparatus. Inset shows exploded view of Broida oven, which was replaced with a low-pressure "boat" heater for the lifetime experiments.

and disappeared for flows greater than 50 scc min^{-1} . In addition, the low oxidant flow ensured that the kinetic processes investigated were mainly due to the buffer gas rather than the F_2/He mixture. The 4-liter cell was evacuated with a $600 \text{ liter min}^{-1}$ pump to guarantee rapid product removal. The pressure in the cell was varied either by changing the buffer gas flow rate or by throttling the vacuum port. Pressure in the chamber is monitored using a capacitance manometer with 10-mTorr resolution.

An excimer pumped dye laser (Lambda Physik EMG 101/FL 2001) is directed into the chamber through baffled side arms to reduce scattered laser light. The dye laser, operating in the region 420-460 nm, is used to selectively excite a specific $\text{BiF A}0^+$ vibronic level by tuning to the bandhead of a particular $\text{A}0^+, v' \rightarrow \text{X}_1 0^+, v''$ transition. The resulting fluorescence was collected by an $\text{F}/1.0$ condenser lens and photomultiplier tube (PMT) [EMI 6236S, "S" (Q) photocathode] orthogonal to the laser beam. Narrowband (1 nm FWHM) interference filters were inserted in front of the PMT to isolate the emission from a single $\text{A}0^+$ state vibrational level. The six filters used had maximum transmission near the heads of the (0,2), (1,3), (1,4), (2,2), (3,5), and (3,7) $\text{A} \rightarrow \text{X}$ bands. The PMT signals were recorded by a 100-MHz transient digitizer (Transiac 2001). A DEC LSI 11/23 laboratory computer averaged the signals from as many as 200 laser shots and stored the results for archival and further analysis.

BiF excitation spectra were obtained by tuning the dye laser and recording the BiF fluorescence with a boxcar integrator (SRS SR280). The narrowband filters were replaced by a long-wave-pass glass filter (Corning 3-71), which enabled BiF emission with wavelengths longer than 500 nm to be detected. The output of the boxcar was digitized with an analog-to-digital converter, and the resulting spectra were stored in the computer.

The temperature of the flame was recorded by a thermocouple and was confirmed, at one pressure, by a rotational line analysis of $\text{BiF}(\text{X}0^+)$ using a cw ring dye laser (Coherent 699-21, linewidth = 20 MHz). The temperature was measured at each experimental pressure (443 K at 1 Torr, -523 K at 8 Torr). In the analysis of kinetic data, the measured temperature was used; however,

no attempt was made to model any slight dependence of the rate coefficients over this range of 485 ± 40 K.

The following materials were used in the experiments without further purification: 10% F_2 in He (Spectra Gases), Ar (Matheson UHP 99.999%), He (Air Products 99.995%), and bismuth metal (Allied Chemical 99.8%).

III. RESULTS

A. BiF A0⁺ RADIATIVE LIFETIME

Decay curves obtained from the time behavior of BiF A0⁺ + X₁O⁺ (v',v'') emission were fit to a single exponential function to determine the radiative lifetime for a particular v' level. The data could be fit to times greater than three lifetimes for all levels. Typical experimental data, along with the fit, are plotted in Fig. 2. For each A state vibrational level studied, runs were made at several pressures ranging from 20 to 50 mTorr. In all cases, the measured lifetimes did not change within the experimental error, indicating that the results are independent of collisional effects. To determine whether radiation trapping was negligible, several runs were performed with increasing BiF density by varying the temperature of the boat heater ± 200 K. Again, the lifetimes remained constant. The results are shown in Table I along with the data for the BiF A state kinetics, which are described in the following subsection. For the A state vibrational levels investigated (v' = 0-3), the measured radiative lifetime is 1.4 ± 0.1 μ s.

B. BiF A0⁺ STATE KINETICS

Following initial laser excitation on a single A + X (v',v'') band, the time derivative of the population of an A state vibronic level can be modeled as

$$\begin{aligned} \frac{dN_{v'}}{dt} = & [1/t_{v'} + M(kq_{v'} + k_{v',v'-1} + k_{v',v'+1})]N_{v'} \\ & + M(k_{v'-1,v'}N_{v'-1} + k_{v'+1,v'}N_{v'+1}) \end{aligned} \quad (1)$$

where N_i is the population of level v', M is the buffer gas concentration, $t_{v'}$ is the radiative lifetime, $kq_{v'}$ is the electronic quenching rate coefficient, and $k_{i,j}$ are the vibrational transfer rates from level i to level j. In this model, multiquanta vibrational transfer collisions are neglected. For BiF A, the time scale of vibrational energy transfer is comparable to the radiative decay for several torr of buffer gas. Electronic quenching, however, is at

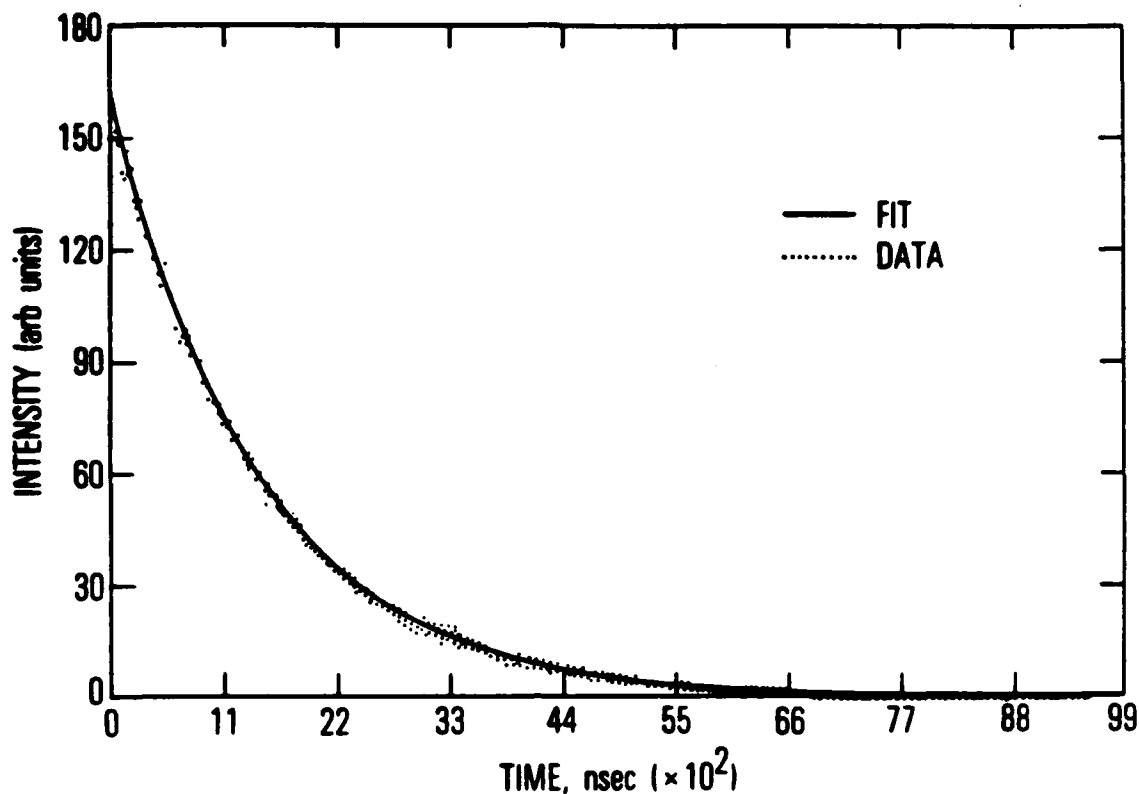


Fig. 2. $\text{BiF}(\text{AO}^+, v' = 0 \rightarrow \text{XO}^+, v'' = 2)$ radiative decay at 30 mTorr He and corresponding single exponential fit. The decay curve is the average of 100 shots. The fit represents a lifetime of 1.44 μs .

TABLE I. Radiative Lifetimes, Electronic Quenching Rate Coefficients, and $V \rightarrow T$ Relaxation Rate Coefficients for $\text{BiF}(\text{AO}^+)^a$

LEVEL	τ_{RAD} (μs)	$\text{BiF}(\text{AO}^+, v \rightarrow \text{AO}^+, v-1)$ ($\text{cm}^3 \text{ molec}^{-1} \text{ s}^{-1}$)		$\text{BiF}(\text{AO}^+, v \rightarrow \text{X}, b, a2)$ ($\text{cm}^3 \text{ molec}^{-1} \text{ s}^{-1}$)	
		Ar	He	Ar	He
$v=0$	1.44			3.8×10^{-13}	3.5×10^{-13}
$v=1$	1.30	1.5×10^{-12}	6.1×10^{-12}	4.3×10^{-13}	3.8×10^{-13}
$v=2$	1.44	5.7×10^{-12}	1.8×10^{-11}	5.0×10^{-13}	4.3×10^{-13}
$v=3$	1.47	1.1×10^{-11}	3.5×10^{-11}	8.1×10^{-13}	5.0×10^{-13}

^aNOTES:

1. Radiative lifetimes quoted to $\pm 0.1 \mu\text{s}$.
2. The error in all rate coefficients is estimated to be $\pm 50\%$ as derived from a sensitivity test of our fitting routine.
3. Pressure ranges: 0 to 8.2 Torr.

least an order of magnitude slower under similar conditions. Under these circumstances, extraction of the quenching and vibrational state-to-state transfer rate constants from the LIF emission time profiles of single $A, v' \rightarrow X, v''$ vibronic bands is not feasible.

In the experiment described here, we initially excite $\text{BiF}(\text{AO}^+, v'=1)$ and the time resolved emission from the $v'=0,1,2,3$ vibrational levels is recorded. The observed emission intensity from level v' is proportional to the population in that level and is given by

$$I_{v'} = G F_{v'} S_{v'} q_{v', v''} N_{v'} \nu^3 \quad (2)$$

where $I_{v'}$ is the emission intensity, G is a constant depending on the detection geometry, $F_{v'}$ is the filter transmission and fractional overlap with the (v', v'') band, $S_{v'}$ is the PMT sensitivity at the wavelength of the (v', v'') band, $q_{v', v''}$ is the Franck-Condon factor for the transition, $N_{v'}$ is the population of level v' , and ν is the transition frequency at the (v', v'') bandhead.

Our analysis required that an internally self-consistent and calibrated data set be generated for each buffer gas pressure. So that relative populations for different vibrational levels could be obtained from the experimental data, the factors appearing in Eq. (2) were determined. The detection geometry was not changed during the experiments, so the factor G is constant for all levels studied. The PMT wavelength sensitivity was calibrated using a tungsten ribbon filament pyrometer lamp (GE SR 8A). The contours of filter transmission curves were measured by passing blackbody radiation through the filters. The transmitted light, along with the emission from an atomic neon lamp for absolute wavelength calibration, was dispersed by a monochromator and imaged on an optical multichannel analyzer (PAR OMA III). This procedure enabled the wavelengths of the transmission peaks to be determined with an estimated error of 0.02 nm. The absolute transmission of the filters was obtained using a Beckman model UV 5240 spectrophotometer. The convolution of the filter transmission curves with the (v', v'') bands was then calculated by

summing the rotational lines for the particular band, weighted by the filter transmission. Assumed was a rotational equilibrium at the temperature in the laser interaction zone as measured with a thermocouple.

To extract the rate coefficients for electronic quenching and V-T transfer, we used a model with parameters $k_{q,v'}$ and $k_{v',v'+1}$ to fit the data for the time-dependent population density. A computer program was written to numerically integrate the rate equations for the vibrational levels studied, namely, $v' = 0-3$. Equation (1) is the general form used. The simultaneous equations are solved using a finite difference calculation of the population $N_{v'}$ for each iteration of the parameters $k_{q,v'}$ and $k_{v',v'+1}$. The rate constants $k_{v'+1,v'}$ were calculated by detailed balance. The values for the radiative lifetimes, $t_{v'}$, are held fixed, since they were determined separately in the low-pressure experiments. Using initial guesses to the parameters $k_{q,v'}$ and $k_{v',v'+1}$, as generated from rise and fall times of the data, the program seeks a set of constants that minimizes chi-squared for the four (v',v'') time profiles at each buffer gas pressure. Figure 3 displays the data for $v' = 0,1,2,3$ and the corresponding numerical fit at a He pressure of 1.5 and 8.2 Torr. The data obtained with Ar buffer gas are comparable. The results are presented in Table I.

The error in the rate coefficients cannot easily be reduced. In this type of analysis, errors to the rate coefficient are known to accumulate for successive v' levels from the initial excitation to $v'=1$, because rate constants determined for a specific v' level are used in calculations for each successive v' level away from $v'=1$. Therefore, in our experiment the rate coefficients (V-T and quenching) for $v'=1$ are best known (have smallest error) followed by those for $v'=0,2$, and 3, respectively. From our parameter sensitivity analysis, we estimate the rate coefficients for $v'=1$ and $v=0$ to be much better than our quoted 1 σ error of $\pm 50\%$. However, the rate coefficients for levels $v'=2$ and 3 are larger and approach $\pm 50\%$.

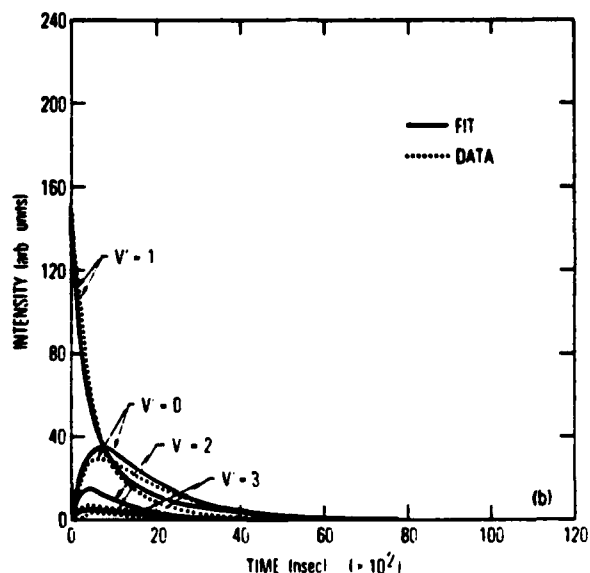
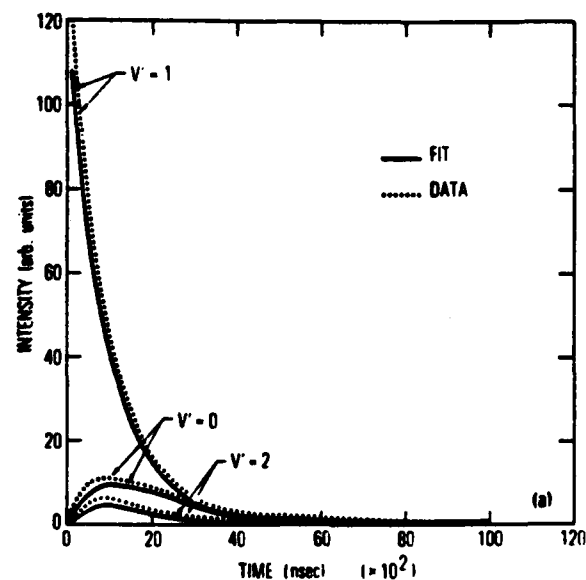


Fig. 3. Time evolution profiles of $\text{BiF}(\text{AO}^+, v' = 0, 1, 2, 3)$ fluorescence following initial excitation to $v' = 1$ at $t = 0$ and their associated numerical fits: (a) 1.5 Torr He, set (b) 8.2 Torr He. Data for $v' = 3$ at 1.5 Torr are relatively small and cannot be drawn on the same scale as fluorescence data from $v' = 0, 1, 2$. At 8.2 Torr the fit to $v' = 2$ shows a larger discrepancy with the data. This anomalous difference cannot be explained and may be due to a calibration error for the particular run. An attempt to force-fit $v' = 2$ data results in gross fits for $v' = 0, 1$, and 3.

IV. DISCUSSION

A. $\text{BiF } A_0^+$ RADIATIVE LIFETIME

The results of our experiments show that BiF may be a good candidate for a visible laser pumped via chemical excitation.⁶ Like the interhalogens, IF ,¹⁵ BrF ,¹⁶ and BrCl ,¹⁷ which have been considered to be particularly promising, $\text{BiF}(A)$ also has kinetic and radiative properties that make it attractive. The measured 1.4- μs $\text{BiF}(A)$ radiative lifetime and the proposed lasing frequency ($\sim 457 \text{ nm}$) make the cross section for stimulated emission for $\text{BiF}(A \rightarrow X)$ somewhat larger than that for $\text{IF}(B \rightarrow X)$.

Recently, an optically pumped $\text{IF}(B \rightarrow X)$ laser, operating in the red, has been demonstrated.¹⁸ The kinetic properties of the $\text{IF}(B)$ are also very similar to our results for $\text{BiF}(A)$.¹⁹ We have found that $\text{BiF}(A)$ electronic quenching is inefficient for He and Ar, and that collisional thermalization within the A state vibrational manifold can be accelerated more than radiative and quenching processes. Therefore, population pumped into the vibronic manifold of $\text{BiF}(A)$ will quickly redistribute to populate low v' states.

For the interhalogen species, such redistribution is a distinct advantage, because these molecules exhibit an equilibrium internuclear separation of the B state that is much greater than that of the X state. This difference causes the most probable radiative transitions from low B, v' states to terminate on high X, v'' levels. Since the equilibrium population of these high v'' states is much less than that of $v''=0$, X state vibration relaxation facilitates establishment and maintenance of a population inversion. In the case of BiF , the shift of equilibrium internuclear separation is not so large: The largest Franck-Condon factors from $\text{BiF}(A, v'=0)$ are to $\text{BiF}(X, v''=0, 1)$ with nearly equal probability.³ Therefore, a BiF laser may have a reduced efficiency caused by partial "bottlenecking" in the ground vibrational states.

Our experiments yielded no variation in the radiative lifetime with increase in v' . The $\text{BiF}(A_0^+)$ state is known to be perturbed by at least two other electronic states that are predicted to emit to the radiatively

metastable a_2 and b_0^+ electronic states.³ Emission to these metastable states will rob population from potential lasing transitions. Spectroscopic analysis has revealed these features to be rotational perturbations that occur at higher v' states ($v' > 5$). Since we did not measure radiative lifetimes from selected rovibronic states, our results reflect an average radiative lifetime for that particular vibrational state. Although rotational perturbations, as evidenced by possible changes in the lifetime, would not be seen in our experiment, our results support the spectroscopic studies in that no change in the radiative lifetime was observed for vibrational levels up to and including $v' = 3$.

B. $\text{BiF } A_0^+$ STATE KINETICS

In Table I, we list the rate coefficients as generated from the multiparameter fit for electronic quenching by Ar and He buffer gas. Argon is slightly more efficient than He in quenching $\text{BiF}(A)$. That Ar is larger and more polarizable could account for the difference.²⁰ Generally, the $\text{BiF}(A)$ electronic quenching rates for Ar and He buffer gas are small and do not compete with the radiative rate for pressures less than 40 Torr. At 8 Torr of buffer gas, the rate of electronic quenching for a vibronic level is 10%-30% of the radiative rate. When compared with existing data for the interhalogens, He quenches $\text{BiF}(A)$ at least an order of magnitude faster than it does $\text{IF}(B)$, for which an upper limit of $1 \times 10^{-14} \text{ cm}^3 \text{ molec}^{-1} \text{ s}^{-1}$ is given.¹⁹ A similar comparison can be made with the quenching of $\text{BrF}(B)$ by Ar, with quenching of $\text{BiF}(A)$ again being faster by an order of magnitude.¹⁶

A trend of increasing electronic quenching with increase in v' was also indicated for both He and Ar buffer gases, a dependence that has been observed in other molecules, such as I_2 ²¹ and IF .¹⁹ Whereas theoretical models for electronic quenching in molecules do not specifically incorporate the vibrational dependence, classical scattering arguments show that in general there is a dependence on electronic quenching with the hard sphere collision diameter, which may be related to a critical-impact parameter b_c found in more developed theories.²² For a harmonic oscillator molecule, one would expect an increase in b_c with increase in v' , and this increase would be larger for the anharmonic $\text{BiF}(A_0^+)$ ($\omega_e = 383.8 \text{ cm}^{-1}$, $\omega_e x_e = 3.5 \text{ cm}^{-1}$). The observed trend of

a general increase in the quenching with v' may support the conclusion that nearby electronic states do not perturb the vibrational levels up to $v'=3$, causing increased quenching at a specific v' . Spectroscopic evidence³ shows that nearby electronic states perturb $\text{BiF}(\text{AO}^+)$ at higher vibrational levels, $v' > 6$.

Table I lists the measured vibrational-to-translational energy transfer rate coefficients. Given that the average vibrational spacing is only 370 cm^{-1} ($\omega_e = 383.8 \text{ cm}^{-1}$), and that under our experimental conditions kT is 363 cm^{-1} ($T = 523 \text{ K}$), the V-T energy transfer rates in $\text{BiF}(\text{A})$ are expected to be fast. This speed is evident in the kinetic studies of $\text{IF}(\text{B})$ in which the downward V-T rates for $v'=3$ and 4 for the He quencher were measured as 5.4×10^{-12} and $6.9 \times 10^{-12} \text{ cm}^3 \text{ molec}^{-1} \text{ s}^{-1}$, respectively.¹⁹ For $\text{IF}(\text{B})$ the average vibrational spacing is 389 cm^{-1} , and in those experiments $kT = 208 \text{ cm}^{-1}$.

Our results show that the V-T rate coefficients for He are larger than those for Ar buffer gas. However, the calculated probability for V-T transfer is the same for both collision partners. The apparent difference largely reflects the difference in the translational velocity between He and Ar. In the fitting of the data for both the $\text{IF}(\text{B})$ studies and our $\text{BiF}(\text{A})$ experiments, the V-T transfers were limited to one quantum of vibration. For an adiabatic collision, the probability of a multiquanta (e.g., $\Delta v=2$) transition was shown by Herman and Shuler²³ to be related to the anharmonicity constant x_e . Using the known constants for $\text{BiF}(\text{A})$, the probability for a $\Delta v=2$ transition is approximately 5×10^{-3} that of a single-quantum transfer. We tested this prediction by including V-T rates for $\Delta v=2$ transitions in our multiparameter fitting routine. The rates for the multiquanta transfer were included as a percentage of the single-quantum rate.

We observed no difference in the fits for the probability of $\Delta v=2$ transition of up to 20%. For high vibrational levels ($v'=23,24,25$) of $\text{I}_2(\text{B})$, the probability of $\Delta v=2$ transitions was measured to be nearly 20%;²⁴ however, at those levels, the vibrational spacing is 165 cm^{-1} , where kT was 284 cm^{-1} . In our experiment, kT is more nearly equal to the energy spacing of the vibrational levels.

Classical models for V-T energy transfer predict that the V-T downward transition rates, $k_{i,i-1}$ from v_i , will scale as v_i for low vibrational levels. In the plot of our state-to-state rate coefficients (Fig. 4), $k_{i,i-1}$ versus v' for both He and Ar buffer gases, the dependence, given by the linear fit, is more $v'^{(1.7)}$ than $v'^{(1.0)}$. We attempted to fit our digitized experimental data to a model that incorporated the classical v' scaling, as discussed by Millikan and White²⁵ and elaborated by Montroll and Shuler.²⁶ The model could reasonably fit LIF emission data from the adjacent $v'=0$ vibrational level following initial excitation to $v'=1$. However, the LIF emission fits to $v'=2$ and $v'=3$ were not as good. We conclude that, using these models for v' scaling of the V-T rates, we cannot comprehensively model the intravibrational relaxation in $\text{BiF}(A, v')$. To date there does not seem to be a satisfactory theoretical model to explain the strong v dependence observed in fast V-R,T processes. Recent results by Dzelzkalns and Kaufman²⁷ on vibrational relaxation of HF/DF ($v'=9-12$, with $\Delta v = 1-1900 \text{ cm}^{-1}$) by HF/DF support our observations. Most of the V-R models suggest that the relaxation is intramolecular, thus permitting V-R in BiF even though the collision partner is monatomic.

To our knowledge these results provide the first excited-state kinetic and lifetime information on the heavier group V A-halogen radical species. Lifetime and some kinetic information is known for the NF^* and PF^* species, but only spectroscopic information is available for AsF^* , SbF^* , and BiF^* . The increasingly complicated spectroscopy--due in part to excited-state perturbations, Hund's case (c) coupling, spin-spin splitting, and the difficulties associated with selectively preparing these species--is at least partially responsible for this lack of data.

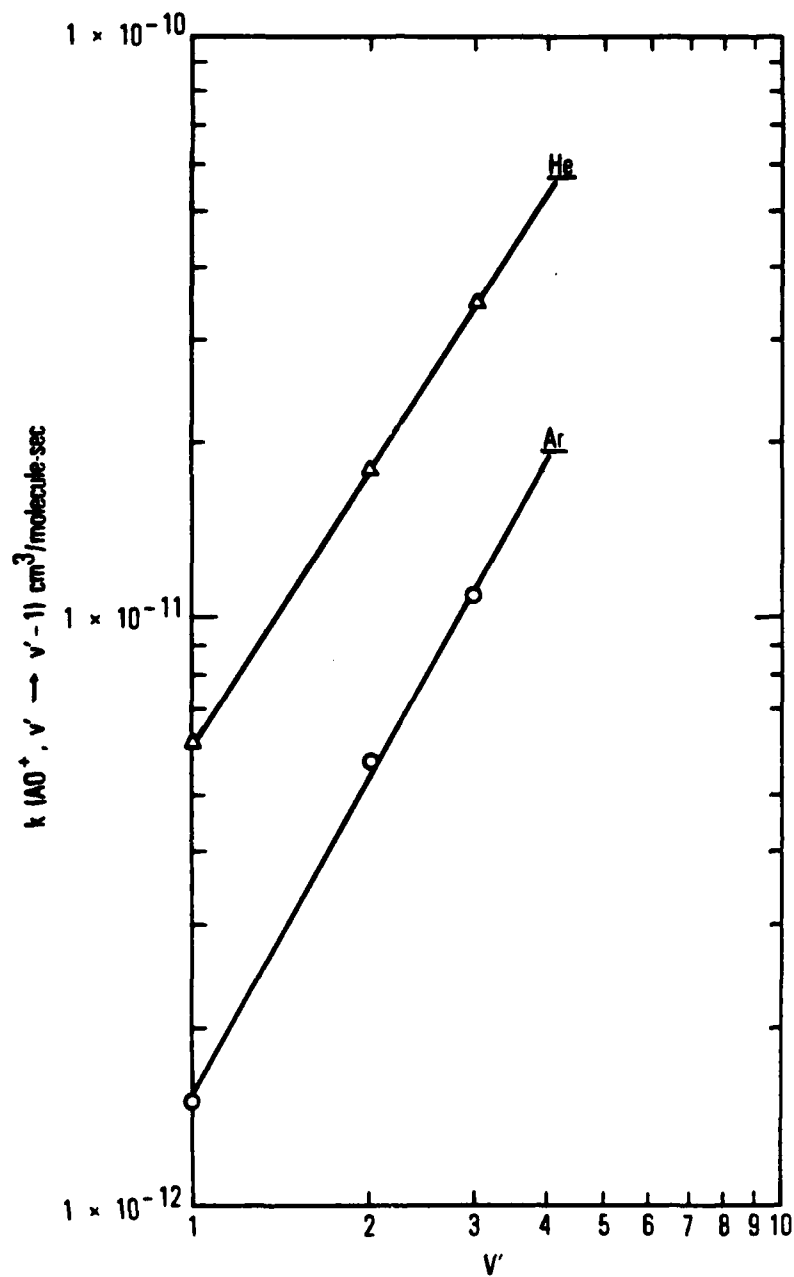


Fig. 4. Measured V-T($k_{1,1-1}$) energy transfer rate coefficients as a function of v' for He and Ar.

V. SUMMARY

An experimental study was performed in which the $\text{BiF}(\text{AO}^+)$ radiative lifetime was measured for several $v'=0-3$, and the electronic quenching and V-T rate coefficients were also measured with the rare gases He and Ar for those v' . The results indicate that Ar is slightly more efficient than He in electronic quenching. For both gases, the quenching-rate constant increases with v' , a result that is predicted from classical models. The quenching rates become competitive with the radiative decay rate only for pressures in excess of 40 Torr. The vibrational relaxation (V-T) rate constants for all levels studied are at least an order of magnitude greater than those for electronic quenching. These rates compete effectively with radiative decay for buffer gas pressures on the order of 3 Torr. Hence, rapid equilibrium within the AO^+ vibrational manifold will occur at moderate pressures followed by a slower decay of this equilibrium, governed by quenching and spontaneous emission. Contrary to the behavior predicted by the classical harmonic oscillator model, the vibrational relaxation rate coefficients are not proportional to v' . The reported V-T rate coefficients scale as $v'^{1.7}$ for both He and Ar, for $v'=0-3$. The measured A state radiative lifetime (1.4 μs) does not vary within experimental error for the v' levels investigated.

REFERENCES

1. H. G. Howell, Proc. R. Soc. London Ser. A 155, 141 (1936).
2. F. Morgan, Phys. Rev. 49, 41 (1936).
3. W. E. Jones and T. D. Mclean, J. Mol. Spectrosc. 90, 481 (1981).
4. K. M. Rao and P. T. Rao, Indian J. Phys. 39, 572 (1965).
5. B. S. Mohanty and K. N. Upadha, Curr. Sci. 36, 478 (1967).
6. J. M. Herbelin and R. A. Klingberg, Int. J. Chem. Kinet. 16, 849 (1984).
7. J. M. Herbelin and N. Cohen, Chem. Phys. Lett. 20, 603 (1973).
8. J. M. Herbelin, Chem. Phys. Lett. 42, 367 (1976).
9. R. W. Field, G. A. Capelle, and M. A. Revelli, J. Chem. Phys. 63, 3229 (1975).
10. C. R. Jones and H. P. Broida, J. Chem. Phys. 60, 4369 (1974).
11. R. Hultgren, R. L. Orr, P. D. Anderson, and K. K. Kelly, Selected Values of Thermodynamic Properties of Metals and Alloys (Lawrence Radiation Laboratory, University of California, Berkeley, 1970), Vol. I.
12. K. J. Chakoo and M. M. Patel, Indian J. Pure Appl. Phys. 17, 189 (1979).
13. C. E. Moore, Atomic Energy Levels, NBS Circular 467, U.S. G.P.O., Washington, DC, 1958.
14. K. P. Huber and G. Herzberg, Molecular Spectra and Molecular Structure: Constants of Diatomic Molecules (Van Nostrand, New York, 1979).
15. M. A. A. Clyne and I. S. McDermid, J. Chem. Soc. Faraday Trans. 2 74, 1644 (1978).
16. M. A. A. Clyne and J. P. Liddy, J. Chem. Soc. Faraday Trans. 2 76, 1569 (1980).
17. M. A. A. Clyne and I. S. McDermid, J. Chem. Soc. Faraday Trans. 2 73, 1094 (1977).
18. S. J. Davis, L. Hanco and R. F. Shea, J. Chem. Phys. 78, 172 (1983).

19. P. J. Wolf, J. H. Glover, L. Hanko, R. F. Shea, and S. J. Davis, J. Chem. Phys. 82, 2321 (1985).
20. A. Dalgarno, Adv. Phys. 2, 282 (1962).
21. J. I. Steinfeld, Acc. Chem. Res. 3, 313 (1970).
22. J. E. Velazco, J. H. Kolts, and D. W. Setser, J. Chem. Phys. 69, 4357 (1978).
23. R. Herman and K. E. Shuler, J. Chem. Phys. 21, 373 (1953).
24. J. I. Steinfeld, J. Chem. Phys. 46, 4550 (1967).
25. R. C. Millikan and D. R. White, J. Chem. Phys. 39, 3209 (1963).
26. E. W. Montroll and K. E. Shuler, J. Chem. Phys. 26, 454 (1957).
27. L. S. Dzelzkalns and F. Kaufman, J. Chem. Phys. 81, 4975 (1984).

END

7-87

DTIC